Electronic tricroscopic examination of the structure of the Ti-50.2 at. % Ni alloy

Nasiba Abduraimova[1*], *Yulbarskhon* Mansurov[2], *Nodirjon* Tursunov[2], and *Uchqun* Rakhimov[2]

[1]Institute of General and Inorganic Chemistry of the Academy of Sciences of the Republic of Uzbekistan, Tashkent, Uzbekistan
[2]Tashkent State Transport University, Tashkent, Uzbekistan

Abstract. The method of electron-microscopic analysis investigated the structure of the alloy Ti-50.2 at % Ni at different stages of dissolution; low-temperature thermomechanical treatment (LTTT), post-deformation edgy (PDE), and recrystallization. The microstructure of B2-austenite, which is formed in the process of incoordination, was also investigated, including in the conditions of isothermic burning of the original recrystallized structure.

1 Introduction

The alloy Ti-50.2 at.%Ni of general technical purpose, widely used for actuators, is weak and occupies an intermediate position in the nickel content between the ecvitom and aging alloy of medical use studied in work. According to well-known data, aging in titanium nickel content with a nickel content of less than 50.5% does not go; however, there is reason to believe that when exposed in the interval of temperatures 400-450° C, it to some extent develops [1-3]. In favor of this assumption are evidenced by the data of the work, which revealed some inhibition of grain growth in the roasting compared to the ageless alloy Ti-50.0 at.%Ni.

It should be noted that in the study of structure formation in the alloy Ti'50.2 at.%Ni, its traditional exposure at a temperature interval of 400-450 °C 1 h, however, the work showed that the alloy Ti-50.7 at.%Ni in a nanostructural state after aging at an optimal temperature of 430°C, 10 h Ti_3Ni_4 phase particles are not visualized but are defined by X-ray and electron [4-7]. There is also no data on the effect of burn-off on the calorimetric effects of martensite transformations in the original crystallized structure.

2 Materials and Methods

The alloy Ti-50.2at%Ni was obtained by vacuum-induction smelting (OPPF oven - 3M) in the "MATEX Industrial Center." Its chemical composition is shown in table 1 electron microscopy.

[1*] Corresponding author: titenash@mail.ru

Table 1 - Chemicals of the Alloy Ti'50.2at%Ni

Element	Ni	Ti	O	C	H	N
Mass share, %	55.2	44.8	0.10	0.037	0.0072	0.009

The sharpened and cropped bar weighing 22 kg and 90-100 mm in diameter was subjected to cross-screw rolling at a temperature of 850-900 ° C to a diameter of 20 mm, followed by cooling in the air; deformation in one pass did not exceed 15%.

Subsequent operations included a sequential edict and rotational force to 2.8 mm (temperature 700° C); dragging to 1.9 mm (temperature 600÷700° C) and burning at 500° C, 1 hour [7-15]. The dragging to 0.4 mm was carried out at a temperature of 450÷500° C, and then the recrystallization was carried out at 700° C. From a diameter of 0.4 mm to 0.3 mm carried out cold dragging to produce the accumulated deformation of 44% (e -0.6). The wire scheme is presented in Figure 1.

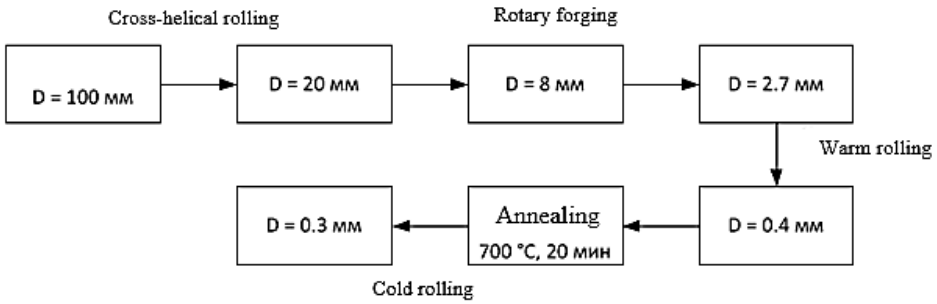

Fig.1 Wire Receiving Scheme

Samples were made from the wire for translucent electron microscopy.

Transmission Electron Microscopy (TEM). Structural studies were carried out at the NUST MISIS Center for Metallurgy and Metallurgy on a JEM-2100 transmission electron microscope (TEM) at an accelerating voltage of 200 kV.

Samples for electron microscopic studies were prepared as follows. Wire segments were poured into a holder with a diameter of 20 mm with conductive casting and polished to the middle of the sample section, then etched in a 1HF + 3HNO3 + 6H2O2 solution to remove the work-hardened layer. Foils from the wire were cut out of samples from the middle using a Strata FIB 205 scanning ion microscope by local precision ion etching using a focused ion beam with an accelerating voltage of 30 kV. Some electron microscopic studies were made from a tape, which was obtained according to the scheme shown in Figure 2.

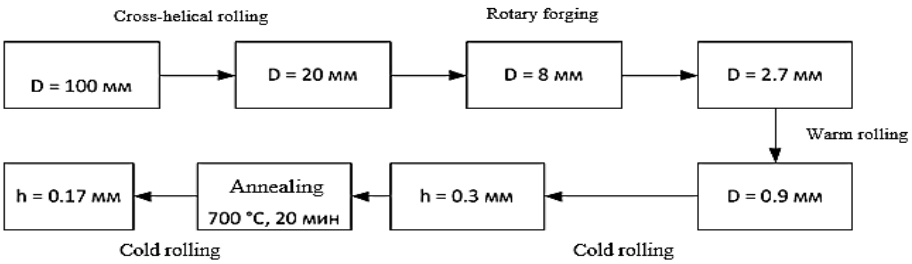

Fig. 2. Scheme of rolling crimping

A wire with a diameter of 0.9 mm was deformed by cold rolling on a laboratory mill DUO 100 in several passes to a thickness of 0.3 mm, then recrystallization annealing was carried out at 700 ° C for 20 minutes, and cold rolling was carried out to obtain a flattened thickness of 0.17 mm; the true accumulated deformation was e = 0.6. Further thinning of foils was carried out on a PIPS II Gatan ion thinning device.

3 Results and Discussion

As a result of cold drawing with accumulated strain e = 0.6, a developed dislocation substructure of B2-austenite is formed, shown in figure 3. A characteristic halo in the diffraction pattern indicates partial amorphization of the structure. The diffraction arcs belong to B2 − austenite; weak reflections of B19′− martensite are determined at high magnification.

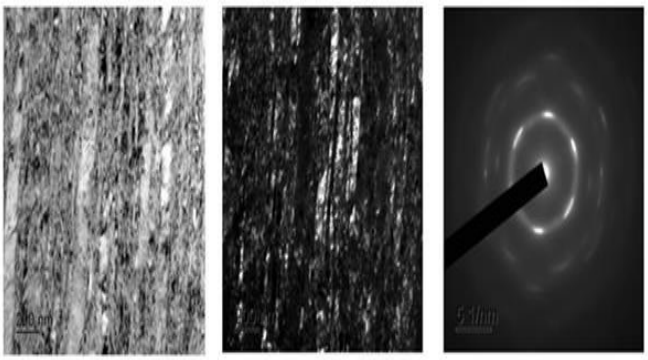

Fig. 3. Microstructure of Ti-50.2 at.% Ni alloy after cold drawing with accumulated strain e = 0.6; zone axis $<111>_{B2}$

The peculiarities of the structure evolution with increasing exposure time make it possible to trace the images shown in figure 4.

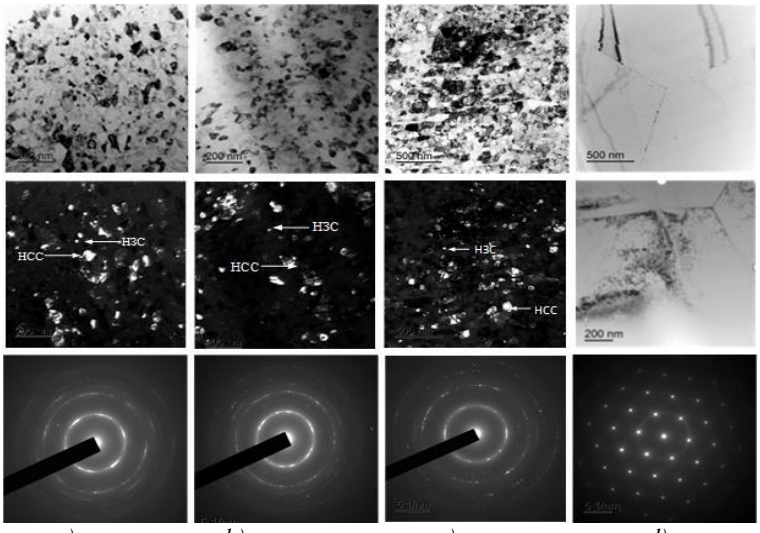

a) *b)* *c)* *d)*

Fig. 4. Microstructure of Ti – 50.2 at.% Ni alloy after cold deformation: a, b - annealing at 430 ° C, a) 1 h; b) 10 h; c) 500 ° C, 1 h; d) 700 ° C, 30 min + 430 ° C, 10 h.

H3C - elements of nanograined structure; HCC - elements of nanosubgrain substructure

Under the conditions of post-deformation annealing at a temperature of 430 ° C, the processes of pre-separation at the zone stage and softening and nanocrystallization of the amorphous component of the austenite structure, proceed simultaneously.

The structure formed as a result of exposure at 430 °C for 1 h consists of a mixture of nanosized subgrains of the polygonized ("nanosubgrained") substructure and grains nano-grained structure of B2-austenite. At the same time, their fractions are comparable (figure 4 a). A similar structure was obtained in the Ti – 50.7 at.% Ni alloy after cold rolling and the same annealing [5, 6]. The average size of structural elements is d = 30 ± 3 nm, the minimum is 10 nm, and the maximum does not exceed 90 nm.

In the dark-field image, nanoscale isolated nanocrystalline grains and extended elongated regions of the polygonized substructure are determined. In the microdiffraction pattern, the superposition of arc reflections from a nanosubgrain structure and point reflections from nanosized grains distributed over a ring is determined (figure 4a). The reflections of the Ti_3Ni_4 phase are not determined.

Longer annealing at the same temperature for up to 10 h leads to an increase in the size of structural elements up to 45 ± 5 nm (Figure 4 b). In the microdiffraction pattern, the fraction of arc reflections decreases, while the fraction of point reflections from recrystallized grains increases. Reflections become clearer and "sparse" due to an increase in the size of structural elements, and their maximum size does not exceed 100 nm. The reflections of the Ti_3Ni_4 phase and at a shorter holding time are not determined.

An increase in the annealing temperature to 500°C for 1 h is accompanied by an increase in the average size of structural elements to d = 67 nm (figure 4c).

Since the structural elements visible in bright-field images cannot be reliably assigned to grains or subgrains, the average size of structure elements was determined d = 67 nm

The histogram of the distribution of structural elements after different processing modes is shown in Figure 5, their average size was d = 45 ± 2 nm, and the maximum size does not exceed 100 nm.

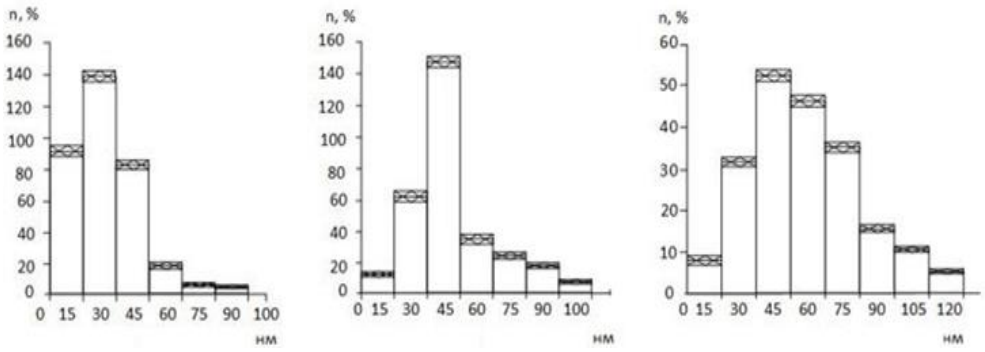

a) *b)* *c)*

Fig. 5. Histograms of the distribution of the size of structural elements after cold deformation: a) 430 °C, 1 h; b) 430 °C, 10 h; c) 500 °C, 1 h

As a result of recrystallization burning at 700 °C, 30 minutes formed a grain structure with grain size~10 microns. Subsequent aging at 430 °C, 10 hours does not result in the release of Ti_3Ni_4 particles (figure 4 d). The observed relief may be the result of processes at

the pre-release stage. The diffractograms determine the reflexes of B2-austenite and R-martins. There are no Ti_3Ni_4 phase reflexes.

4 Conclusion

1. The cold dragging of Ti 50.2 at.% Ni with accumulated deformation e 0.6 forms a developed dislocation substructure B2-austenite with partial amorphization. As a result of post-deformation, a nanostructure consisting of suberized polygonized substructure and recrystallized grains, the size of which increases with the temperature and time of burning, is formed. As a result of burning at 700 °C has formed a recrystallized structure B2-austenite with the size of grain 10 microns.

2. As a result of burning at 430 °C, 10 h. of alloy with the original and recrystallized structure of the Ti_3Ni_4 phase particles are not released, their presence is not electronically determined.

References

1. Huang W., On the selection of shape memory alloys for actuators, Mater. Design **23** (1) pp 9-11 (2002).
2. Leary M., Huang S., Ataalla T., Baxter A., Subic A., Design of shape memory alloy actuators for direct power by an automotive battery, Mater. Design **43**, pp 460-466. (2013)
3. V. Brailovski, S. Prokoshkin, K. Inaekyan, V. Demers. Functional properties of nanocrystalline, submicrocrystalline and polygonized Ti-Ni alloys processed by cold rolling and post-deformation annealing. Journal of Alloys and Compounds **V.** 509 (5). pp. 2066–2075. (2011).
4. K. Inaekyan, V. Brailovski, S. Prokoshkin, A. Korotitskiy, A. Glezer Characterization of amorphous and nanocrystalline Ti-Ni-based shape memory alloys. Journal of Alloys and Compounds, .**473**, Issue (1-2), pp.71-78. (2009).
5. K. Polyakova, E. Ryklina, S. Prokoshkin. Thermomechanical response of titanium nickelide on austenite grain/subgrain size Materials Today: Proc. Pp 4836−4840. (2017).
6. K.A. Polyakova-Vachiyan, E.P. Ryklina, S.D. Prokoshkin, S.M. Dubinskii. Dependence of the Functional Characteristics of Thermomechanically Processed Titanium Nickelide on the Size of the Structural Elements of Austenite. Phys. Met. Metallogr. **117** (8) pp 817−827. (2016).
7. S.D. Prokoshkin, V. Brailovski, K.E. Inaekyan, V. Demers, I.Yu. Khmelevskaya, S.V. Dobatkin, E.V. Tatyanin. Structure and properties of severely cold-rolled and annealed Ti–Ni shape memory alloys Mater. Sci. Eng. A pp. 114–118. (2008)
8. I.Yu. Khmelevskaya, S.D. Prokoshkin, V. Brailovski, K.E. Inaekyan, V. Demers, I.B. Gurtovaya, A.V. Korotitskiy, S.V. Dobatkin. Functional properties of Ti–Ni based shape memory alloys. Advances in Science and Technology **V**. (59) pp. 156−161. (2008).
9. V. Brailovski, S. Prokoshkin, I. Khmelevskaya, K. Inaekyan, V. Demers, S. Dobatkin, E. Tatyanin. Interrelations between the properties and structure of thermomechanically treated equiatomic Ti–Ni alloy. Mater. Sci. Eng. A V. pp. 597–601. (2006)
10. X. Wang, S. Kustov, B. Verlinden, J. V. Humbeeck. Fundamental Development on Utilizing the R-phase Transformation in NiTi Shape Memory Alloys. Shape Mem. Superelasticity V.**1**. № (2). pp 231–239. (2015).

11. M.S. Shakeri, J. Khalil-Allafi, V. Abbasi-Chianeh, Arash Ghabchi. The influence of Ni_4Ti_3 precipitates orientation on two-way shape memory effect in a Ni-rich NiTi alloy. JALCOM 485 pp. 320–323. (2009)
12. Ching-Yig Chang, David Vokoun, and Chen-Ti Hu. Two-way shape memory effect of NiTi alloy induced by constraint aging treatment at room temperature, Metallurgical and Materials Transactions a. V. (32). july (2001) pp. 1629 – 1634. (2001).
13. X.L. Meng, W. Cai, Y.D. Fu et al. Shape-memory behaviors in an aged Ni-rich TiNiHf high temperature shape-memory alloy. Intermetallics (16) pp 698–705. (2008).
14. Z. Wang, X.Zu, X. Feng, J. Dai. Effect of thermomechanical treatment on the two-way shape memory effect of NiTi alloy spring. Materials Letters (554) pp. 55–61. (2002)
15. E.P. Ryklina, S.D. Prokoshkin, A.Y. Kreytsberg. Abnormally high recovery strain in Ti-Ni-based shape memory alloys. Journal of Alloys and Compounds 577 pp 255−258. (2013)
16. 1.Adilkhodjaev, A., Shaumarov, S., Kadir, U. New structure assessment method cell concrete. International Journal of Advanced Science and Technology, **29** (5), pp. 1889-1893.(2020)
17. 8.Shaumarov S.S., Adilhodzhaev A.I., Shipacheva E.V., Kandkhorov S.I. Development of New Constructive and Heat-Insulating Materials. International Journal of Recent Technology and Engineering (IJRTE). ISSN: 2277-3878. **7**. Issue-(5).. pp. 577-580. (2019)
18. 7.Shaumarov S.S., Adilhodzhayev A.I., Kondrazhenko V.I. Experimental research of structural organization of heat-insulating structural building materials for energy efficient buildings. XXII International Scientific Conference on Advanced In Civil Engineering «Construction the formation of living environment», pp. 1-7 (2019)
19. 5.Adilhodzhaev A.I., Shaumarov S.S., Makhamataliev I.M., Tsoy V.M. Features Of Forming The Structure Of Cement Concrete On Second Crushed Stone From Concrete Scrap, International Journal of Advanced Science and Technology **29**, No. (5), pp. 1901-1906.(2020).
20. 3.Adilhodzhayev A., Shaumarov S., Shipacheva E., Shermuhamedov U. New method for diagnostic of heat engineering and mechanical properties of cellular concrete, International Journal of Engineering and Advanced Technology (IJEAT) ISSN: 2249 – 8958, Volume-**9** Issue-(1), October 2019. – pp. 6885-6887. (2019).
21. Adilhodzhayev A. I., Shaumarov S.S., Umarov K.S. New Structure Assessment Method Cell Concrete, International Journal of Advanced Science and Technology. **29**, (5), pp. 1889-1893. (2020).